



UNIVERSITY OF LEEDS

This is a repository copy of *Hot melt extrusion of heat-sensitive and high melting point drug: Inhibit the recrystallization of the prepared amorphous drug during extrusion to improve the bioavailability.*

White Rose Research Online URL for this paper:

<https://eprints.whiterose.ac.uk/181014/>

Version: Accepted Version

Article:

Huang, D, Xie, Z, Rao, Q et al. (6 more authors) (2019) Hot melt extrusion of heat-sensitive and high melting point drug: Inhibit the recrystallization of the prepared amorphous drug during extrusion to improve the bioavailability. *International Journal of Pharmaceutics*, 565. pp. 316-324. ISSN 0378-5173

<https://doi.org/10.1016/j.ijpharm.2019.04.064>

© 2019, Elsevier. This manuscript version is made available under the CC-BY-NC-ND 4.0 license <http://creativecommons.org/licenses/by-nc-nd/4.0/>.

Reuse

This article is distributed under the terms of the Creative Commons Attribution-NonCommercial-NoDerivs (CC BY-NC-ND) licence. This licence only allows you to download this work and share it with others as long as you credit the authors, but you can't change the article in any way or use it commercially. More information and the full terms of the licence here: <https://creativecommons.org/licenses/>

Takedown

If you consider content in White Rose Research Online to be in breach of UK law, please notify us by emailing eprints@whiterose.ac.uk including the URL of the record and the reason for the withdrawal request.



eprints@whiterose.ac.uk
<https://eprints.whiterose.ac.uk/>

Hot melt extrusion of heat-sensitive and high melting point drug: Recrystallization of prepared amorphous drug during extrusion process

Deen Huang,^{a,b} Evangelos Liasas,^c Shixia Guan,^b Zhenyu Jason Zhang,^c Ming Lu,^{a*} and Qingguo Li^{b**}

^aSchool of Pharmaceutical Sciences, Sun Yat-Sen University, Guangzhou 510006, China

^bSchool of Pharmaceutical Sciences, Guangzhou University of Chinese Medicine, Guangzhou 510006, China

^cCentre for Formulation Engineering, School of Chemical Engineering, University of Birmingham, B15 2TT, U.K.

^dFirst Clinical Medical College, Guangzhou University of Chinese Medicine, Guangzhou 510006, China

ABSTRACT

Transforming crystalline drug to amorphous state and then extruding into ASD at temperature below T_m is an effective method to extrude heat-sensitive and high melting point drug. However, in this work, we observed recrystallization of prepared amorphous tadalafil (TD) during extrusion, which lead to failure in ASD extrusion. The recrystallization process of amorphous TD during extrusion and reheating process were investigated in details. The results indicated that spray-dried TD sample is much easier to recrystallize (occurred from 150°C) in comparison to the melt-quenched TD sample (recrystallized from 190°C). Huge surface area of spray-dried sample might be the cause of its poor stability. As a result, extruding Soluplus and spray-dried amorphous TD at 160°C yielded amorphous solid dispersion (ASD) at 10% drug loading and crystalline solid dispersion above 20% drug loading. The method that spray drying 20% TD with 80% Soluplus and then extruding the spray-dried sample can obtain ASD at 20% drug loading at 160°C, 142°C lower than the melting point of TD (302°C). This sample showed higher degree of release, better physical stability and higher bioavailability (in rats) compared to spray-dried sample and hot-melt extruded sample using Soluplus and spray-dried TD. This optimal formulation exhibited bioavailability 1.6-fold higher than the commercial Cialis® (in dogs).

Keywords: Hot melt extrusion, heat-sensitive, high melting point, recrystallization, amorphous solid dispersion, tadalafil

Introduction

Hot melt extrusion (HME) is an extensively used method to prepare amorphous solid

* Corresponding author, Ming Lu, E-mail: luming3@mail.sysu.edu.cn, ORCID ID: 0000-0002-2622-1528.

** Corresponding author, Qingguo Li, E-mail: lqg8512@gzucm.edu.cn.

dispersion (ASD) for the improvement of dissolution and bioavailability of water-insoluble drug. Extrusion temperature is usually higher than the melting point (T_m) of the drug to yield an ASD product[1] unless the polymer carrier can strongly interact with drug and thus depress the T_m of drug[2, 3]. However, many drugs are heat-sensitive, degrading upon or even before melting [2, 3]. What's more, some drugs have very high T_m ($>200^\circ\text{C}$), at which most pharmaceutical polymers thermally degrade [4]. For example, ivacaftor melts and bubbles at 291°C , while etravavine degrades upon melting at 246°C (observed in our lab, data not shown). Therefore, how to extrude chemically stable ASD for a heat-sensitive and high melting point drug is a big issue.

In our previous work[5], carbamazepine ASD was successfully extruded at 160°C (30°C lower than its T_m , 190°C) by cocrystallizing carbamazepine with nicotinamide (T_m , carbamazepine-nicotinamide cocrystal= 160°C). Haser *et al.* [2] observed that PVP VA64 can suppress the T_m of meloxicam from 255°C to 175°C , but significant chemical degradation (confirmed as hydrolysis) was detected when processing above 140°C . Screw design and barrel configuration were optimized to drive-off moisture and reduce melt residence time, achieving 96.7% purity. Then, meglumine was added to provide a stabilizing basic microenvironment, successfully resulting in 100% purity. However, these methods are only effective for special drugs, which have functional groups (usually hydrogen bonding receptor or acceptor) and can strongly interact with polymer carriers [2, 3] or cocrystal co-formers [5]. Lakshman *et al.*[6] reported a method, in which the heat-labile drug was firstly transformed into amorphous form using solvent evaporation and then extruded as ASD at the temperature much lower than its T_m . This method has no special requirement about the drug's functional group and seems to have more extensive application. However, one issue should be taken into account. That is the possible recrystallization of amorphous drug during extrusion process, especially for the drugs having strong crystallization tendency.

Crystallization tendency of pharmaceutical compound was classified by Taylor's group[7], ranked as Class IA > Class IB > Class II > Class III. Class III compounds have very good glass stability and recrystallize very slowly. They can be directly liquefied during reheating process without recrystallization (for example indomethacin and celecoxib, observed in our lab, data not shown). However, Class I and II compounds have strong crystallization tendency. Their amorphous materials usually recrystallize when passing a certain temperature range at cooling or reheating process, where nucleation rate and crystal growth rate get a balance. However, the phase behavior of amorphous Class I and II compounds during reheating process is extremely

complicated [8-11] and poorly understood.

Tadalafil (TD) is the first-line drug for the treatment of erectile dysfunction and pulmonary arterial hypertension. It belongs to Biopharmaceutics Classification System Class II drug [12] with a poor solubility lower than 5 $\mu\text{g/mL}$ [13]. Several literatures reported the solubilization of TD using ASD technique prepared by spray drying [14, 15], freeze drying [16], ball milling [14, 17, 18], solvent evaporation [12, 19, 20] and HME [13]. This compound has very high T_m (299°C) [13], poor thermal stability and strong crystallization tendency (belongs to crystallization tendency Class II compound, data not shown). Therefore, TD was selected as the model drug.

The aim of the present work is to study how to prepare ASD by HME for such a thermally labile and high melting point compound and understand more about the phase behavior of amorphous compound with strong crystallization tendency during HME process.

2. Materials and Methods

2.1. Materials

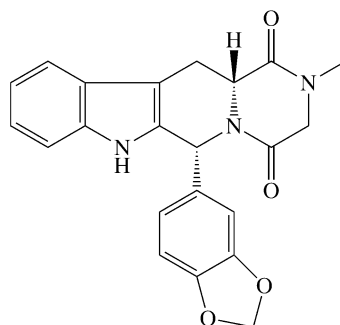


Figure 1. Chemical structure of tadalafil

TD was kindly donated by Haotian Co. (Gansu, China). Standard substances of TD and sulfamethoxazole (Internal Standard, IS) were purchased from National Institutes for Food and Drug Control (Beijing, China). Soluplus[®] was kindly donated by BASF SE (Ludwigshafen, Germany). HPLC-grade acetonitrile and formic acid were purchased from Merck & Co., Inc. (Darmstadt, Germany) and Fisher Scientific Inc. (San Jose, USA), respectively. Acetone and all other reagents were analytical grade chemicals.

2.2 Methods

2.2.1 Differential Scanning Calorimeter (DSC)

Thermal behavior of TD, physical mixtures and solid dispersions was investigated using a NETZSCH DSC (NETZSCH 200 F3 Maia, Netzsch Gerätebau, Selb, Germany). Samples (5-10 mg) were accurately weighed into the aluminum pans, sealed and heated at 10°C/min under a nitrogen purge.

2.2.2 Powder X-ray Diffraction (XRPD)

Crystalline state of samples was characterized using PXRD (D8 Advance Bruker, Germany) with Cu K α radiation, operating at 40 kV and 40 mA. The 2 θ range was 5–35° with a scanning rate of 5°/min.

2.2.3 Spray drying

One milligram of TD or TD/Soluplus physical mixtures (at 10%, 20%, 30% and 40% drug loadings) equivalent to 1 mg TD were dissolved in 100 mL acetone/water solvent (9:1, v/v). Spray drying was performed with a Mini Spray Dryer B-290 (Buchi, Switzerland). Inlet temperature was 85°C, resulting in an outlet temperature of 60°C. Solution pump speed was 9% (6 mL/min) and aspirator was operated at 100%. The TD/Soluplus ASD products were named as S10, S20, S30 and S40, as listed in **Table 1**.

Table 1. Formulations, drug content and process parameters of TD/Soluplus solid dispersions

Formulations	Drug loading (%)	Drug content (%)	Preparation methods
S10	10	10.22	TD/Soluplus ASD prepared by spray drying.
S20	20	21.03	
S30	30	31.53	
S40	40	40.60	
SE10	10	11.33	Amorphous TD was firstly spray-dried and then hot-melt extruded with Soluplus at 160°C.
SE20	20	21.84	
SE30	30	28.83	
SE40	40	39.23	
co-SE10	10	9.52	TD/Soluplus ASD was spray-dried and then hot-melt extruded at 160°C.
co-SE20	20	19.92	
co-SE30	30	28.52	
co-SE40	40	41.48	

2.2.4 Hot-melt extrusion

Spray-dried TD/Soluplus ASD or amorphous TD blended manually with Soluplus at different drug loadings (10%, 20%, 30% and 40%) were fed into hot-melt extruder (HAAKE MiniCTW micro compounder, Thermo Electron GmbH, Karlsruhe, Germany). The extrusion temperature was set as 160°C and the screw speed was fixed at 100 rpm. The products were named according to the pretreatment of the materials as listed in **Table 1**. The samples were milled and passed through 120 mesh sieve for further analysis.

2.2.6. Scanning Electron Microscope (SEM)

Scanning Electron Microscope measurements were carried out with a ZEISS EVO 18 electron microscope (ZEISS Co., Germany) at 15 kV and 15 µA. Samples were coated with gold before measurement.

2.2.7. Drug dissolution test under non-sink condition

Dissolution profiles of TD and TD/Soluplus solid dispersions under non-sink condition were tested in pure water. Eight milligram of TD or solid dispersions/physical mixtures equivalent to 8 mg TD were suspended in 50 ml of pure water and shaken at 37 °C/70 rpm for 24 h. One milliliter of samples was withdrawn at predefined time interval of 5 min, 10 min, 20 min, 30 min, 1 h, 2 h, 4 h and 24 h, and then filtered through 0.45 µm polyester filters. The filtrate was diluted by equal volume of acetonitrile to avoid precipitation and analyzed by Accela UHPLC system (Thermo Scientific Inc., San Jose, USA). Each test was carried out in triplicate.

2.2.8. Drug dissolution test under sink condition

Dissolution test under sink condition was performed using a USP paddle dissolution apparatus (ZRS-8G dissolution tester, TiandaTianfa Technology Co. Ltd, Tianjin, China) at a paddle rotation speed of 50 rpm. Samples equivalent to 3 mg of TD were accurately weighed and added to 1000 mL pure water with 0.2% Sodium dodecyl sulphate (SDS). One milliliter of samples were withdrawn at different time points (5, 10, 20, 30, 45 and 60 min) and then filtered through 0.45 µm polyester filters. Another 1 mL of fresh dissolution fluid was added to maintain a constant dissolution volume. The filtrate was subjected to HPLC quantification by Accela UHPLC system (Thermo Scientific Inc., San Jose, USA). Each test was performed in triplicate.

2.2.9. Pharmacokinetic studies in SD Rats

Male Sprague-Dawley (SD) rats, weighing 180-220 g, were purchased from Animal Research Center of Guangzhou University of Chinese Medicine (Guangdong, China). The rats were fasted overnight (about 12 h) before oral administration. Water was provided *ad libitum* throughout experiments. Thirty-two SD rats were randomly divided into 4 groups: (1) TD ($n=8$); (2) S20 ($n=8$); (3) SE ($n=8$); (4) co-SE ($n=8$). All groups were orally administered by gavage with a single dose of 1.8 mg/kg. Following pre-determined time intervals (0.5, 1, 2, 4, 8, 12 and 24 h) after drug administration, 300 μ L blood was drawn from the retro-orbital plexus of the rats, collected in heparinized tubes. The blood sample was immediately centrifuged at 3000 \times g for 15 min at 4 $^{\circ}$ C (Himac CR22, Hitachi, Japan) to obtain the plasma and then stored at -80 $^{\circ}$ C for further analysis.

2.2.10. Pharmacokinetic studies in Beagle Dogs

Male Beagle dogs, weighing 9-11 kg, were purchased from Guangzhou General Pharmaceutical Research Institute Co., Ltd. (Guangdong, China). Six dogs were randomly assigned to two groups of three animals in a two-period cross over design for the oral administration of Cialis[®] and self-made co-SE20 tablet. The washout period between each kinetic study was 1 week. Each dog was orally administered with a single dose of 20 mg TD. Water was available *ad libitum* throughout the experiments. Blood (1.5 mL) were collected in heparinized tubes at predefined time interval of 0.25, 0.5, 1, 2, 3, 4, 8, 12, 24, 36 and 48 h after administration. Each sample was immediately centrifuged at 3000 \times g (Himac CR22, Hitachi, Japan) for 15 min and stored at -80 $^{\circ}$ C until analysis.

2.2.11 Chromatographic quantification methods

For the assay of TD in pharmacokinetic studies, 100 μ L plasma samples was mixed with 10 μ L sulfamethoxazole-acetonitrile solution (2.5 μ g/mL) or 10 μ L acetonitrile in a 1.5 mL tube by vortexing for 1 min. Then, 1000 μ L ethyl acetate was added and vortexed for 3 min. The mixture was centrifuged at 17000 \times g (Himac CR22, Hitachi, Japan) for 15 min at 25 $^{\circ}$ C and then 900 μ L supernatant was transferred into a new 1.5 mL tube, followed by evaporating under nitrogen. The residues were dissolved in mobile phase (100 μ L) and centrifuged at 17000 \times g for 15 min at 25 $^{\circ}$ C (Himac CR22, Hitachi, Japan). Three milliliter of supernatant was injected into the LC-MS.

The Accela UHPLC was performed using a Thermo Hypersil BDS C18 column (2.4 μm diameter particles; 50 mm \times 2.1 mm internal diameter; Thermo Scientific, USA) at 4°C. The composition of mobile phase was 0.1% formic acid aqueous solution (mobile phase A) and acetonitrile (mobile phase B) with a flow rate of 0.4 mL/min. The mobile phase gradient was shown in supporting information (**Table S1**). The injection mode was partial loop and the injection volume was 3 μL .

The mass spectrometric detection was performed on a TSQ Quantum Access Max triple quadrupole mass spectrometer (Thermo Scientific, San Jose, USA) using a heated electrospray ion source (HESI II) in positive ionization mode. Quantification was carried out using selected reaction monitoring (SRM) of the transitions, tube lens voltage and collision energy were m/z 390.2nd col, 98V and 14v for TD and m/z 254.1n ener, 91V and 16v for sulfamethoxazole (IS), respectively, with scan time of 200 ms per transition. The optimized ion source parameters for monitoring analysis were as follows: Spray voltage, 3500V; Vaporizer temperature, 350°C; Capillary temperature, 350°C; Sheath gas, 30arb; Aux gas, 15arb and Q1 FWHM, 0.4amu, respectively.

2.2.12. Pharmacokinetic and statistical analysis

Pharmacokinetic analysis of the data was carried out by noncompartmental methods using WinNonlin software version 5.0.1 (Pharsight Corporation, Mountain View, CA, USA). The maximum concentration of TD after oral administration (C_{max}) and the time taken to reach maximum concentration (T_{max}) were determined from the experimental data. The relative bioavailability was calculated by the ratio of the $AUC_{0-\infty}$ of test sample to the $AUC_{0-\infty}$ of reference.

2.2.13. Physical stability studies

Physical stability of TD solid dispersions was studied by placing samples in opened vials at 40°C and 75% relative humidity (RH). Physical state of the samples was characterized with PXRD (D8 Advance Bruker, Germany).

3 Results and Discussion

3.1 Recrystallization of amorphous TD during HME process

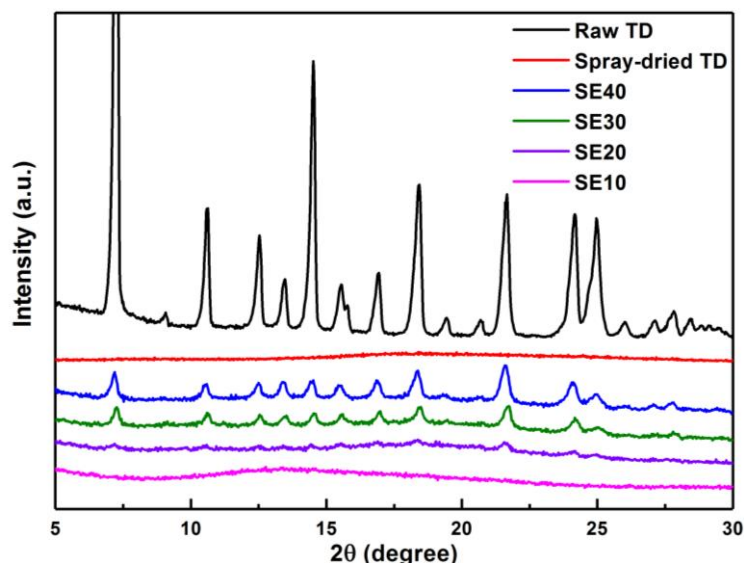


Figure 2. PXRD patterns of TD/Soluplus solid dispersions.

It is difficult to directly extrude amorphous solid dispersion using raw crystalline TD and Soluplus due to the super-high T_m of TD. Krupa *et al.*[13] extruded TD-soluplus solid dispersions at 160°C. As drug loading is higher than 20%, crystalline solid dispersions were obtained. Even at 10% drug loading, some tiny diffraction peaks of TD can be observed in PXRD patterns. Considering high dose in commercial Cialis[®], high drug loading TD ASD is desired.

Inspired by Lalkshman's work[6], crystalline TD was firstly transformed to amorphous TD by spray drying, which was confirmed by PXRD (Figure 2). Then, the amorphous TD was blended with Soluplus at different drug loadings (10%, 20%, 30% and 40%) and extruded at 160°C. Surprisingly, only extrudates with 10% drug loading exhibited classical amorphous PXRD pattern (Figure 2), reflecting ASD was obtained. When drug loading is higher than 20%, diffraction peaks of crystalline TD ($2\theta = 7.3, 10.6, 12.5, 13.5, 14.5, 15.6, 15.8, 16.9, 18.4, 21.7, 24.2$ and 25.0°) were observed in the PXRD patterns of extrudates and the intensity of diffraction peaks increased with increased drug loading, reflecting the increasing crystallinity. These results indicated that amorphous TD pre-prepared by spray drying recrystallized during HME process.

The recrystallization of amorphous drug during extrusion was firstly reported in the present work. The mechanism was poorly understood and thus further investigated. We

prepared amorphous TD sample between two cover slides using melt quenching and then hold it at 160°C (the processing temperature in HME). Surprisingly, it kept as supercooled liquid for 30 min without nucleation occurring and only few nuclei were observed after 40 min (**Figure 3-A**). If melt-quenched sample was heated at 10°C/min, it nucleated from 185°C and completely crystallized at 215°C (**Figure 3-B**). These results indicated that the temperature from 185°C to 215°C is proper to nucleate and grow crystal for amorphous TD prepared by melt quenching. Holding at 160°C for 30 min wouldn't result in recrystallization of TD for melt quenching sample, which is quiet different from the phenomenon in HME.

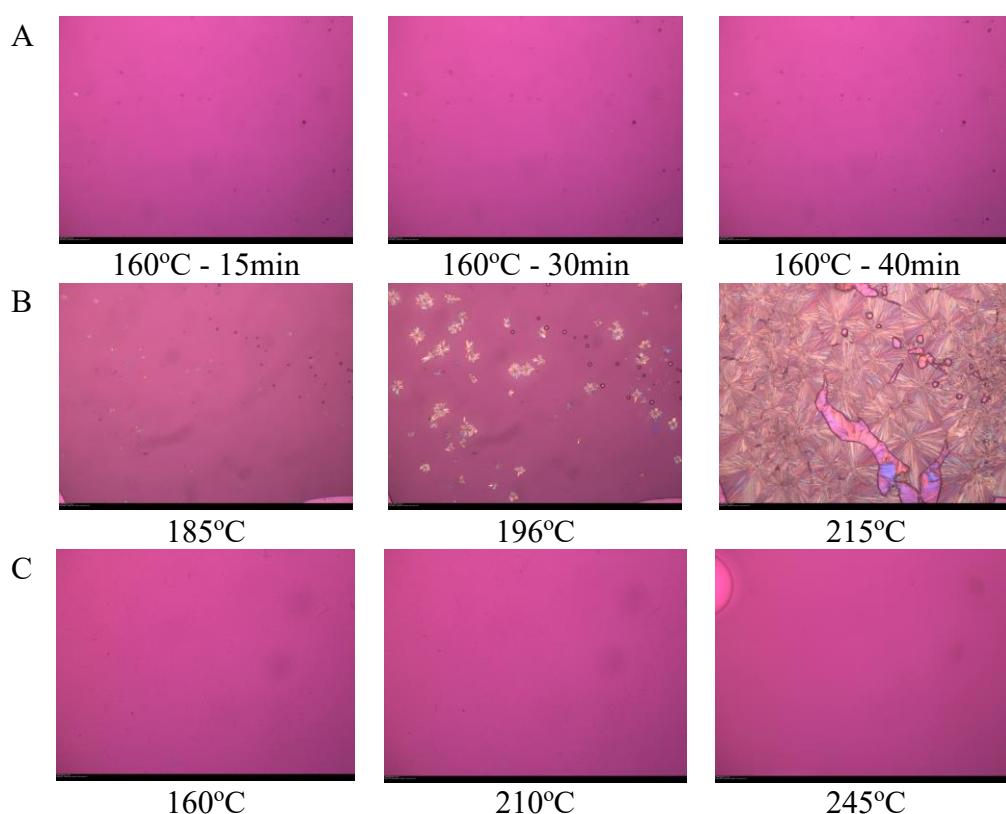


Figure 3. POM images of (A) amorphous TD reheated at 10°C/min; (B) amorphous TD holding at 160°C for different time; (C) 30% TD/Soluplus ASD reheated at 10°C/min. All samples were prepared between two cover slides by melt quenching.

There are two differences between POM and HME reheating process. One is the additional shear force in HME. Another is the preparation of amorphous TD. The amorphous TD used in HME was prepared by spray drying, which has much smaller particle size and higher surface area than melt-quenched samples. The difference in surface area might be the factor resulting in different recrystallization behaviors.

Considering the difficulty in observing crystallization behavior of spray-dried sample using POM, DSC was employed to compare the crystallization behaviors of spray-dried and melt-quenched amorphous TD samples.

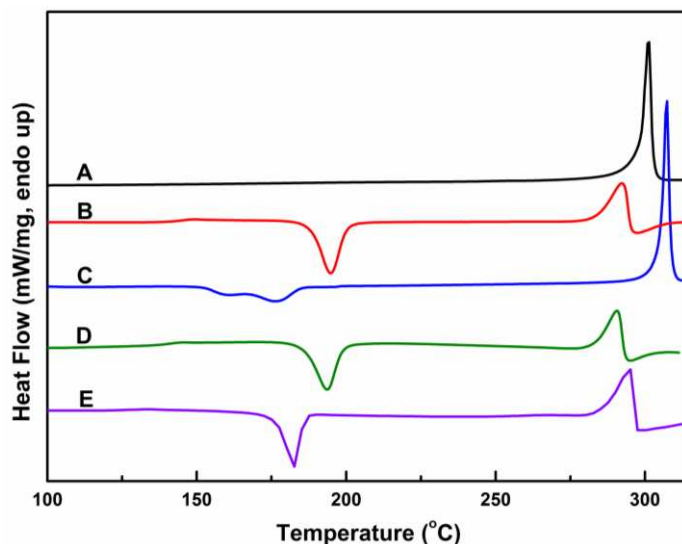


Figure 4. DSC curves of (A) raw and amorphous TD; (B) bulk amorphous TD prepared by melt quenching using raw TD; (C) powder amorphous TD prepared by spray drying; (D) bulk amorphous TD prepared by melt quenching using spray-dried TD; (E) powder amorphous TD prepared by melt quenching and then manually grinding.

As shown in **Figure 4A**, crystalline TD exhibited a melting peak with the peak temperature of 302°C and the melting enthalpy of 101 J/g, which is in good agreement with reported values[18, 21]. In **Figure 4B**, the melt-quenched amorphous TD, prepared in DSC pan, showed a glass transition temperature (T_g) of 144°C and then an exothermic peak corresponding to recrystallization with the onset temperature of 189°C and the peak temperature of 196°C. The newly formed crystal finally melted around 292°C (peak temperature) with $\Delta H_m=67$ J/g. The result indicated that amorphous TD has a very strong tendency to crystallize.

As shown in **Figure 4C**, the spray-dried amorphous TD initiated the recrystallization from 151°C, much earlier than melt quenching sample. The recrystallization exhibited two peaks around 159°C and 174°C. Huge surface area and residual solvent might account for the depression of recrystallization temperature. To exclude the influence of residual solvent on the crystallization behavior of amorphous TD, the spray-dried sample was further dried in vacuum at ambient temperature for different duration and then reheated at 10°C/min. The results indicated that vacuum drying slightly accelerate the recrystallization of amorphous TD (**supporting information Figure S1**) and thus possible residual solvent can't accelerate the recrystallization of amorphous TD. Then, the spray-dried powder sample was then melted in DSC pan at 305°C for 10 s and quenched into bulk sample. This melt-quenched sample exhibited the recrystallization peak around 196°C, close to the melt-quenched sample prepared using raw TD (**Figure 4D**). HPLC data indicated that no thermal degradation occurred during the melting process (data not shown). Therefore, the phenomenon that spray-dried sample

recrystallizes at much lower temperature than melt-quenched sample was ascribed to the huge surface area of the former. To confirm this conclusion, melt-quenched TD samples were prepared on the surface of cover slide and then ground into fine powder with the particle size much smaller than melt-quenched bulk sample but bigger than spray-dried sample. DSC results indicated the melt-quenched powder sample exhibited moderate crystallization onset temperature and peak temperature of 178°C and 184°C, respectively, located between those of melt-quenched bulk sample and spray-dried powder sample (**Figure 4E**). The above results indicated that crystallization temperature of amorphous TD highly depends on the particle size and surface area of the samples (**Figure 5**). The molecules on the surface have higher molecular mobility than the molecules in the bulk[22]. Therefore, higher surface area means more high-energy molecules on the surface, which favors recrystallization at lower temperature. As surface area increases, the crystallization onset temperature decreased from 189°C (melt-quenched samples) to 151°C (spray-dried samples), falling in the common extrusion temperature range. Consequently, recrystallization of spray-dried TD occurred during extrusion process even if Soluplus might have recrystallization inhibition effect.

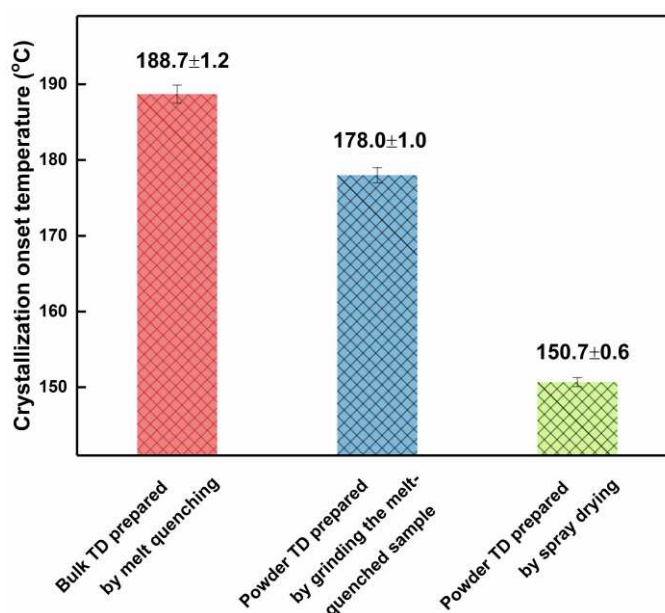


Figure 5. Crystallization onset temperature of amorphous TD prepared by different methods when heating at 10°C/min ($n=3$)

We also prepared TD-Soluplus ASD at 30% drug loading between two cover slides by melt quenching and then observed its crystallization behavior during reheating process. The results were puzzled that the melt-quenched sample was directly liquefied without recrystallization (**Figure 3C**), which is quietly different from the recrystallization of melt-

quenched neat TD and also the fact that spray-dried amorphous TD recrystallized from 30% TD/Soluplus physical mixture in HME process at 160°C. The result hinted that Soluplus can effectively inhibit the recrystallization of amorphous TD (we also obtain TD/Soluplus ASD at 10% drug loading as shown in **Figure 2**) and highly contact between Soluplus and amorphous TD might strengthen this crystallization inhibition effect.

3.2 Spray drying TD with Soluplus and then extruding

Based on the above results, Soluplus was added to the solution and co-spray dried with TD at various drug loadings (10%, 20%, 30% and 40%), yielding TD/Soluplus ASD (**Figure 6-A**). Then, the spray-dried samples were extruded at 160°C. Highly intact between TD and Soluplus strengthened the crystallization inhibition of Soluplus. PXRD results indicated that TD-Soluplus extrudates with 20% drug loading was amorphous sample (**Figure 6-B**). At drug loading of 30% and 40%, Soluplus cannot effectively inhibit the recrystallization of TD in extruder and thus partial solid dispersions were obtained (**Figure 6-B**).

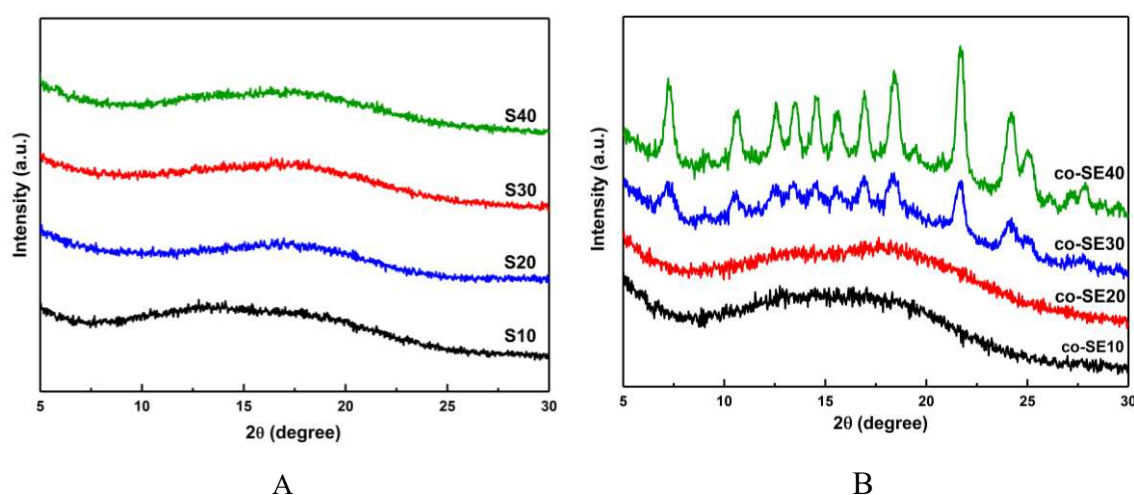


Figure 6. PXRD patterns of TD/Soluplus solid dispersions.

The method that spray-drying TD with soluplus and then extruding the powder sample can yield ASD with higher drug loading (20% drug loading) in comparison to the method that extruding the physical mixture of Soluplus and spray-dried TD (10% drug loading). We selected solid dispersions at 20% drug loading to compare the influence of the two HME methods on the microstructure and the pharmaceutical properties of the extrudates. Spray-dried ASD was also investigated for comparison. As shown in **Figure 7**, SEM and AFM images revealed that S20, the spray-dried sample, exhibited smooth surface and homogeneous morphology, indicating that TD was molecularly dispersed in Soluplus. This high contact between TD and Soluplus helps Soluplus to inhibit the recrystallization of TD during HME process. Consequently, co-SE20 exhibited very smooth morphology and very small phase size.

Conversely, the surface of SE20 was very rough (SEM image) with obvious phase separation (AFM image) in accordance with its partial crystalline state (Figure 2). These differences in microstructure might result in different *in-vitro* dissolution behavior and *in-vivo* pharmacokinetics.

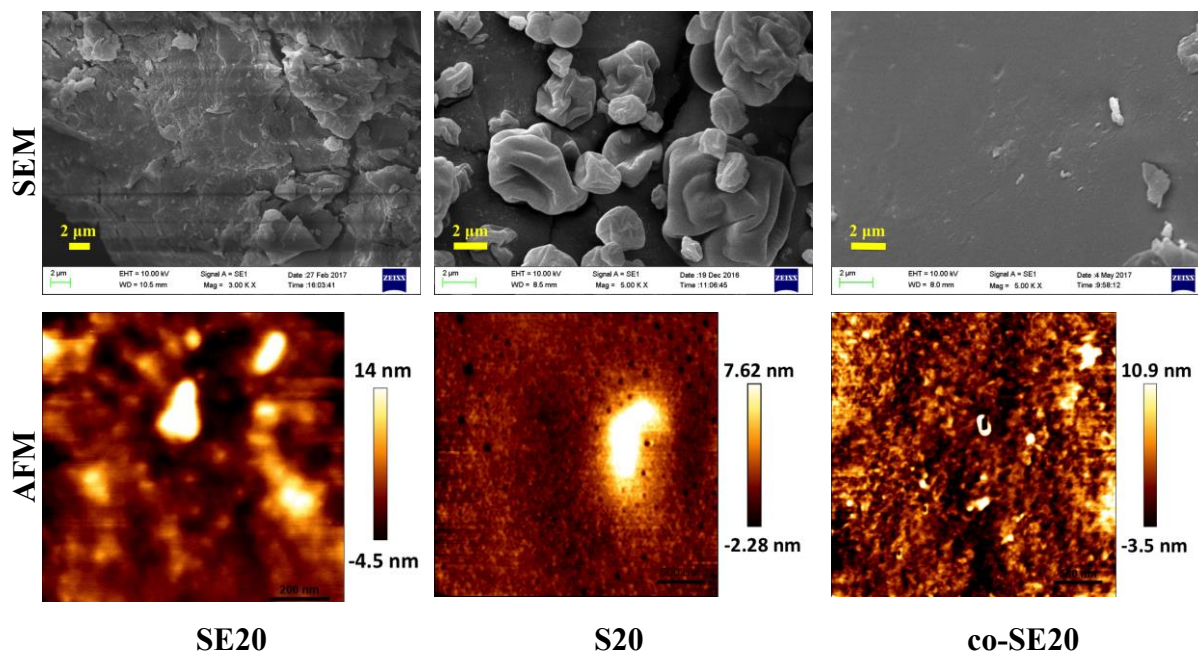


Figure 7. SEM and AFM images of TD/Soluplus solid dispersions.

3.2 In-vivo dissolution profiles

3.2.1 Dissolution profiles under non-sink condition

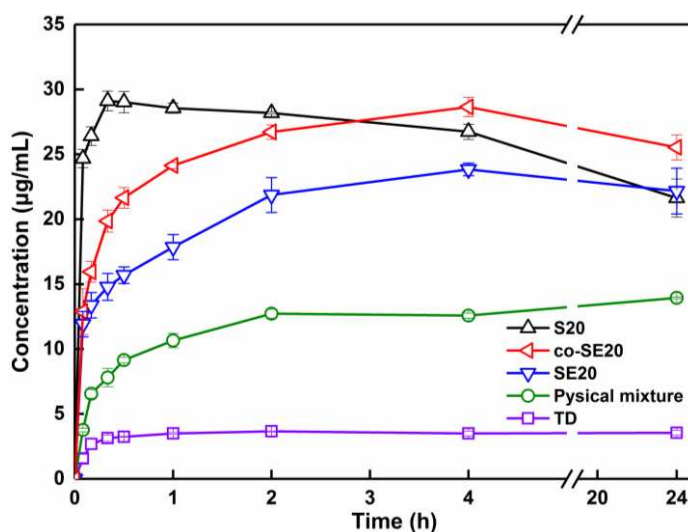


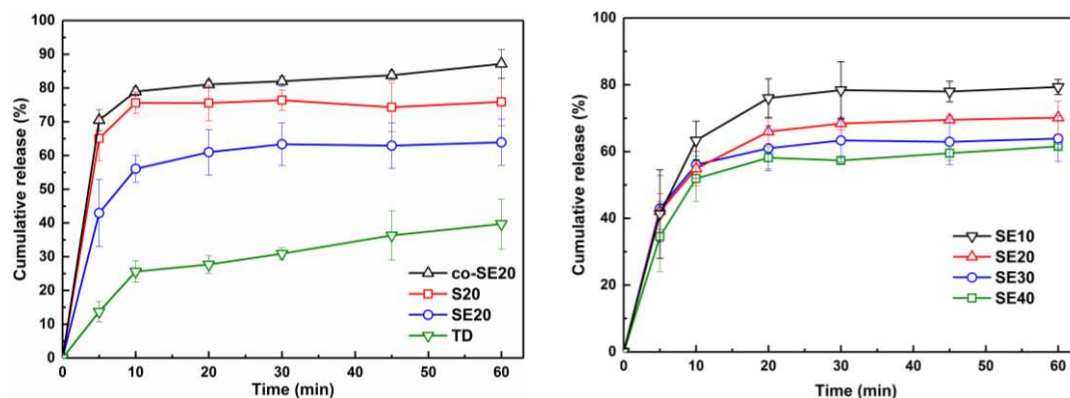
Figure. 8 Release profiles of TD, TD/Soluplus physical mixture and its solid dispersions under non-sink conditions (20% drug loading, $n=3$, mean \pm SD).

Non-sink dissolution profiles of ASD samples with 20% drug loading were investigated.

Eight microgram TD or solid dispersion/physical mixture samples equivalent to 8 mg TD were suspended in 50 ml pure water and shaken for 24 h. All powder samples can't dissolve completely. Raw TD achieved its equilibrium solubility of 3.54 $\mu\text{g/ml}$ after 2 h, close to the reported solubility of 2.8 $\mu\text{g/ml}$ [21], 3 $\mu\text{g/ml}$ [16] and 7.72 $\mu\text{g/ml}$ [23]. For physical mixture of TD and Soluplus, TD dissolved very slowly and achieved 13.94 $\mu\text{g/ml}$ after 24 h, indicating that Soluplus can solubilize TD with a 3.94-fold enhancement at this weight ratio. SE20 achieved 23.84 $\mu\text{g/ml}$ at 4h and then slightly decreased to 22.17 $\mu\text{g/ml}$ after 24h due to the recrystallization of TD. S20 has the fastest release, benefiting from its huge surface area. The drug concentration achieved the peak value of 29.11 $\mu\text{g/ml}$ after 20 min, but then continuously decreased and dropped to 21.63 $\mu\text{g/ml}$ at 24 h. co-SE20 exhibited slower release than S20, but the concentration progressively increased and achieved 28.65 $\mu\text{g/ml}$ at 4 h. After 24 h, the concentration dropped to 25.45 $\mu\text{g/ml}$. Among the three formulations, co-SE20 gave the optimal release profile under non-sink conditions. It might be attributed to the high contact between soluplus and TD and then Soluplus can effectively inhibit the recrystallization of TD from the supersaturated solution.

3.2.2 Dissolution profile under sink condition

Dissolution profile of TD and TD/Soluplus samples under sink condition were evaluated by adding 3 mg TD or samples equivalent to 3 mg TD into 1000 ml pure water with 0.2% SDS. The results were shown in **Figure 9**. Raw TD only dissolved 67.74% after 60 min due to its strong hydrophobicity and high lattice energy (very high T_m of 302°C and melting enthalpy of 39.33 J/mol). All solid dispersions exhibited improved release rate and percentage in comparison of raw TD. For each solid dispersion, the improvement decreased with increasing drug loading. S20, SE20 and co-SE20 exhibited release percentage of 75.92%, 70.17% and 87.19% after 60 min, respectively. The dissolution degree was ranked as co-SE20>S20>SE20, in good agreement with the results of non-sink dissolution.



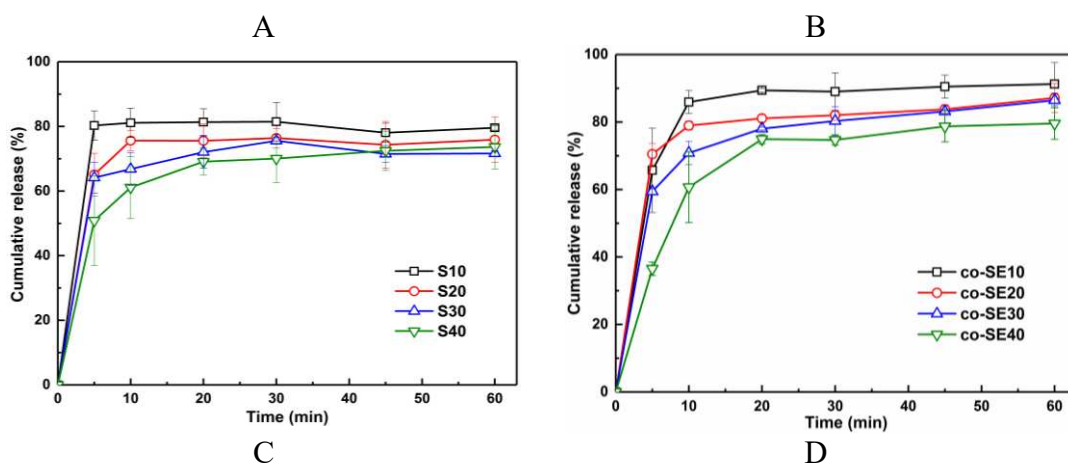


Figure 9. Dissolution profiles of (a) raw TD and TD/Soluplus solid dispersions at 20% drug loading; (b) SE; (c) S; (d) co-SE. ($n=3$, mean \pm SD)

3.3 In-vivo studies

3.3.1 In-vivo studies in SD Rats

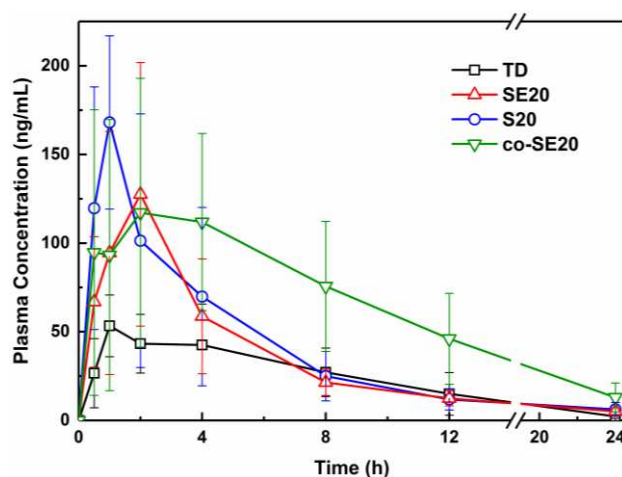


Figure 10. Plasma concentration profiles of TD in rats after oral administration. All formulations were administered in aqueous suspensions. ($n=8$, mean \pm SD)

Table 2. Pharmacokinetic parameters of raw TD and formulations after oral administration in rats ($n = 8$, mean \pm SD)

PK parameter	TD ^a	SE20	S20	co-SE20 ^a
$t_{1/2}$ (h)	4.46 ± 1.07	8.97 ± 5.46	7.10 ± 3.53	7.22 ± 4.22
T_{max} (h)	2.00 ± 1.55	1.56 ± 0.62	1.19 ± 0.53	3.75 ± 2.52
C_{max} (ng/ml)	58.00 ± 15.33	138.52 ± 80.40	182.01 ± 49.66	154.02 ± 63.53
AUC_{0-24h} (ng/ml·h)	488.06 ± 252.36	687.73 ± 267.33	779.54 ± 299.31	1377.36 ± 526.35
$AUC_{0-\infty}$ (ng/ml·h)	503.28 ± 255.41	764.57 ± 317.28	842.72 ± 307.19	1549.39 ± 511.01
MRT_{0-24h}	6.56 ± 0.98	5.67 ± 0.63	5.33 ± 0.81	7.67 ± 1.06
Relative bioavailability	1	1.519	1.674	3.079

^a $n=6$.

Three ASD formulations with 20% drug loading (SE20, S20, co-SE20) were selected for the *in-vivo* studies in SD rats. Pure TD was studied as a control formulation. The powder of formulations was suspended in water and gavage. The mean plasma concentration-time profiles after oral administration were shown in **Figure 10**. The calculated pharmacokinetic parameters were listed in **Table 2**. The results showed that all solid dispersion formulations significantly improved $AUC_{0-\infty}$ and C_{max} of TD compared to raw TD. S20, prepared by spray drying, reached highest C_{max} of 182.01 ± 49.66 ng/ml in shortest T_{max} of 1.19 ± 0.53 h. This result is in good agreement with the *in-vitro* dissolution results and can be attributed to the huge surface area, which led to fast dissolve and then rapid absorption, but also fast elimination (short $t_{1/2}$ of 7.10 ± 3.53 h) and thus low AUC_{0-24h} of 779.54 ± 299.31 ng/ml·h. SE20 exhibited moderate T_{max} (1.56 ± 0.62 h) and longest $t_{1/2}$ (8.97 ± 5.46 h), but lowest C_{max} (138.52 ± 80.40 ng/ml) and AUC_{0-24h} (687.73 ± 267.33 ng/ml·h) among three formulations. It might be attributed to the partially crystalline TD in solid dispersion, which might act as nuclei to accelerate recrystallization of TD from supersaturated solution in GI tract. For co-SE20, the plasma concentration reached C_{max} of 154.02 ± 63.53 ng/ml at T_{max} of 3.75 ± 2.52 h and then decreased slowly. This formulation has highest AUC_{0-24h} of 1377.36 ± 526.35 ng/ml·h and highest relative bioavailability of 3.079 among three formulations.

3.3.2 *In-vivo* studies in Beagle dogs

The optimal formulation, co-SE20, was compressed into tablets with the excipients shown in **Table 3**. Every tablet contains 20 mg TD. The co-SE20 tablet and commercial Cialis® tablet were orally administrated in Beagle dogs at the dose of 20 mg to compare the bioavailability of TD in the two formulations. The average plasma concentration-time profiles were shown in **Figure 11**. The calculated pharmacokinetic parameters were listed in **Table 4**. The C_{max} and the AUC_{0-24h} of the co-SE20 tablet were 1.86-fold and 1.82-fold higher than those of the commercial Cialis® tablet, respectively. The T_{max} of the two formulations were comparable. The $t_{1/2}$ of co-SE20 tablet was 12.82 ± 1.88 h, shorter than that of the Cialis® tablet (18.70 ± 9.21 h). The oral bioavailability of TD in the co-SE20 tablet exhibited 1.691-fold increase in comparison to the commercial Cialis® tablet.

Table 3. Formulation of co-SE20 tablet

Formulation	Weight per tablet (mg)	Tablet weight (mg)	TD dose (mg)
Co-SE20	100	350	20

Copovidone (Kollidon® CL-SF)	17.5
Aerosil®	3.5
Microcrystalline cellulose PH301®	229

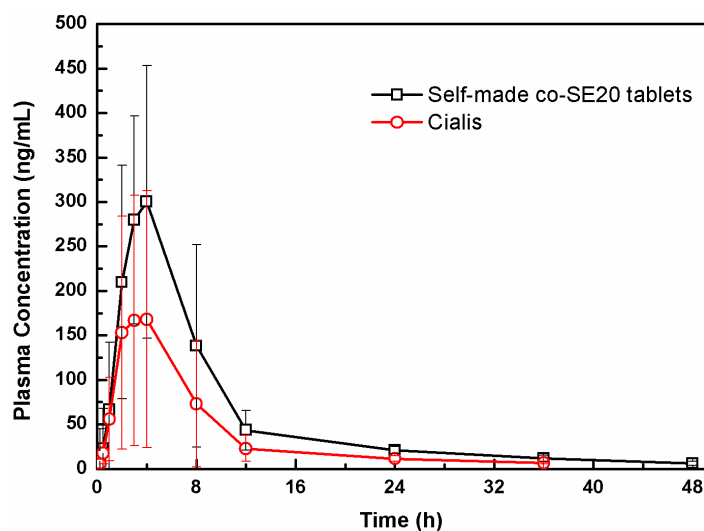


Figure 11. Plasma concentration profiles of TD in Beagle dogs after oral administration of Cialis® and self-made co-SE20 tablets. ($n=6$, mean \pm SD)

Table 4. Pharmacokinetic parameters of Cialis® and co-SE20 tablets after oral administration in Beagle dogs ($n=6$, mean \pm SD)

PK parameters	Cialis®	Co-SE20 tablets
$t_{1/2}$ (h)	18.70 \pm 9.21	12.82 \pm 1.88
T_{max} (h)	3.50 \pm 2.35	3.33 \pm 0.82
C_{max} (ng/ml)	179.73 \pm 140.03	334.70 \pm 138.24
AUC_{0-48} (ng/ml·h)	1441.48 \pm 954.50	2630.69 \pm 1107.23
$AUC_{0-\infty}$ (ng/ml·h)	1623.28 \pm 876.79	2745.71 \pm 1149.07
MRT_{0-48h}	9.66 \pm 2.97	10.25 \pm 2.14
Relative bioavailability	1	1.691

3.4 Physical stability

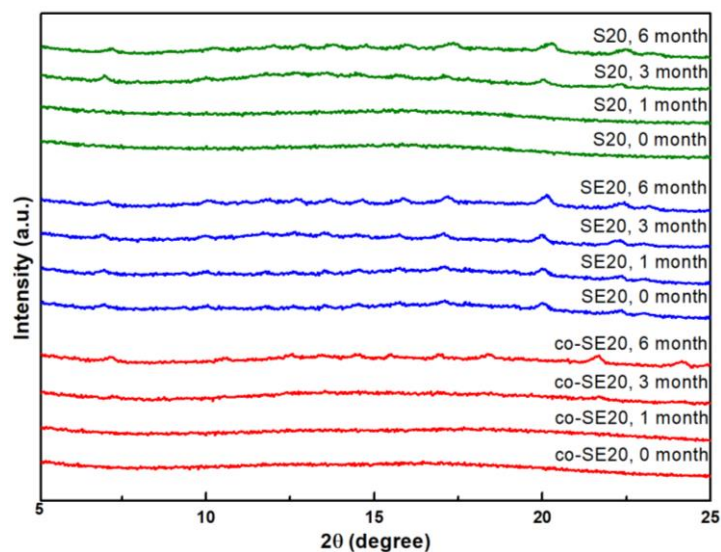


Figure 12. PXRD patterns of S20, SE20 and co-SE20 after storage at 40°C/75% RH.

Solid dispersions with 20% drug loading were subjected to accelerated stability testing. The samples were stored at 40°C/75% RH for 1, 3, and 6 months. The physical state was investigated using PXRD. As shown in **Figure 12**, TD in fresh SE20 sample is partially in crystalline state. During the storage, the crystallinity slightly increased. In fresh S20 and co-SE20 samples, TD was in completely amorphous state. After 3 months, TD began to recrystallize in both formulations. But the crystallinity of TD in co-SE20 significantly lower than that in S20, indicating better physical stability of co-SE20 compared to S20. This result is in good agreement with the POM experiment results that spray-dried sample is easier to recrystallize in comparison to melt-quenched sample. Combined the animal study results with the physical stability results, co-SE20 was considered as the optimal formulations.

The method that spray drying drug with polymer and then extruding into ASD was proved to be an effective method to extrude chemically stable ASD for heat-sensitive and high melting point drug, which has strong crystallization tendency.

4. Conclusions

Transforming crystalline drug to amorphous state and then extruding into ASD at temperature below T_m is an effective method to extrude heat-sensitive and high-melting-point drug. However, recrystallization during extrusion might lead to failure in ASD extrusion for the drugs with strong crystallization tendency (Class I and II). The present work investigated the recrystallization process of amorphous tadalafil (TD) during extrusion and reheating process.

The results indicated that spray-dried TD sample recrystallized much earlier during the heating process due to huge surface area. Spray drying TD with Soluplus at the ratio of 2:8 and then extruding the powder sample can effectively inhibit the recrystallization of TD and obtain ASD at 160°C, 142°C lower than T_m of TD (302°C). This ASD sample exhibited higher release degree, better physical stability and higher bioavailability (in rats) compared to spray-dried ASD sample and hot-melt extruded sample using Soluplus and spray-dried TD. This optimal formulation exhibited the bioavailability, 1.695-fold higher than the commercial Cialis® (in dogs).

References:

1. James C. DiNunzio, F.Z., Charlie Martin, James W. McGinity, *Melt Extrusion, in Formulating Poorly Water Soluble Drugs*, A.B.W. Robert O. Williams III, Dave A. Miller, Editor. 2012, Springer: New York. p. 311-362.
2. Haser, A., et al., *An approach for chemical stability during melt extrusion of a drug substance with a high melting point*. International Journal of Pharmaceutics, 2017. **524**(1-2): p. 55-64.
3. Guo, Z.F., et al., *The utilization of drug-polymer interactions for improving the chemical stability of hot-melt extruded solid dispersions*. Journal of Pharmacy and Pharmacology, 2014. **66**(2): p. 285-296.
4. LaFountaine, J.S., J.W. McGinity, and R.O. Williams, 3rd, *Challenges and Strategies in Thermal Processing of Amorphous Solid Dispersions: A Review*. AAPS PharmSciTech, 2016. **17**(1): p. 43-55.
5. Liu, X., et al., *Improving the Chemical Stability of Amorphous Solid Dispersion with Cocrystal Technique by Hot Melt Extrusion*. Pharmaceutical Research, 2012. **29**(3): p. 806-817.
6. Lalkshman, J.P., et al., *Application of Melt Extrusion in the Development of a Physically and Chemically Stable High-Energy Amorphous Solid Dispersion of a Poorly Water-Soluble Drug*. Molecular Pharmaceutics, 2008. **5**(6): p. 994-1002.
7. Baird, J.A., B. Van Eerdenbrugh, and L.S. Taylor, *A Classification System to Assess the Crystallization Tendency of Organic Molecules from Undercooled Melts*. Journal of Pharmaceutical Sciences, 2010. **99**(9): p. 3787-3806.
8. Lu, M. and L.S. Taylor, *Vemurafenib: A Tetramorphic System Displaying Concomitant Crystallization from the Supercooled Liquid*. Crystal Growth & Design, 2016. **16**(10): p. 6033-6042.
9. Mahieu, A., et al., *On the polymorphism of griseofulvin: Identification of two additional polymorphs*. Journal of Pharmaceutical Sciences, 2013. **102**(2): p. 462-468.
10. Zhang, S., et al., *Impact of Crystal Structure and Polymer Excipients on the Melt Crystallization Kinetics of Itraconazole Polymorphs*. Crystal Growth & Design, 2017. **17**(6): p. 3433-3442.
11. Desgranges, C. and J. Delhommelle, *Molecular mechanism for the cross-nucleation between polymorphs*. Journal of the American Chemical Society, 2006. **128**(32): p. 10368-10369.
12. Choi, J.S. and J.S. Park, *Design of PVP/VA S-630 based tadalafil solid dispersion to enhance the dissolution rate*. Eur J Pharm Sci, 2017. **97**: p. 269-276.

13. Krupa, A., et al., *In vitro and in vivo behavior of ground tadalafil hot-melt extrudates: How the carrier material can effectively assure rapid or controlled drug release*. Int J Pharm, 2017. **528**(1-2): p. 498-510.
14. Wlodarski, K., L. Tajber, and W. Sawicki, *Physicochemical properties of direct compression tablets with spray dried and ball milled solid dispersions of tadalafil in PVP-VA*. Eur J Pharm Biopharm, 2016. **109**: p. 14-23.
15. Wlodarski, K., et al., *Physical stability of solid dispersions with respect to thermodynamic solubility of tadalafil in PVP-VA*. Eur J Pharm Biopharm, 2015. **96**: p. 237-46.
16. Wlodarski, K., et al., *Physicochemical properties of tadalafil solid dispersions - Impact of polymer on the apparent solubility and dissolution rate of tadalafil*. Eur J Pharm Biopharm, 2015. **94**: p. 106-15.
17. Krupa, A., et al., *High energy ball milling and supercritical carbon dioxide impregnation as co-processing methods to improve dissolution of tadalafil*. Eur J Pharm Sci, 2016. **95**: p. 130-137.
18. Krupa, A., et al., *High-Energy Ball Milling as Green Process To Vitriify Tadalafil and Improve Bioavailability*. Mol Pharm, 2016. **13**(11): p. 3891-3902.
19. Choi, J.S., et al., *Tadalafil solid dispersion formulations based on PVP/VA S-630: Improving oral bioavailability in rats*. Eur J Pharm Sci, 2017. **106**: p. 152-158.
20. Choi, J.S., et al., *Use of acidifier and solubilizer in tadalafil solid dispersion to enhance the in vitro dissolution and oral bioavailability in rats*. Int J Pharm, 2017. **526**(1-2): p. 77-87.
21. Wlodarski, K., et al., *The influence of amorphization methods on the apparent solubility and dissolution rate of tadalafil*. Eur J Pharm Sci, 2014. **62**: p. 132-40.
22. Wu, T. and L. Yu, *Surface crystallization of indomethacin below T-g*. Pharmaceutical Research, 2006. **23**(10): p. 2350-2355.
23. Mehanna, M.M., A.M. Motawaa, and M.W. Samaha, *In sight into tadalafil - block copolymer binary solid dispersion: Mechanistic investigation of dissolution enhancement*. International Journal of Pharmaceutics, 2010. **402**(1-2): p. 78-88.